A Vertical Finite-Difference Scheme Based on a Hybrid $\sigma-\theta-p$ Coordinate

ZHENGXIN ZHU,* JOHN THUBURN, AND BRIAN J. HOSKINS

Department of Meteorology, University of Reading, Reading, United Kingdom

PETER H. HAYNES

Department of Applied Mathematics and Theoretical Physics, University of Cambridge, Cambridge, United Kingdom

(Manuscript received 11 December 1990, in final form 16 July 1991)

ABSTRACT

A vertical discretization of the primitive equations in a general vertical coordinate is described that enables a primitive equation model to use terrain-following sigma levels near the ground and isentropic levels higher up, with a smooth transition region in between. Therefore, it combines many of the advantages of the computational efficiency of σ coordinates and the predictive and diagnostic potential of θ coordinates, and should be particularly useful for general circulation models to be used for studies of stratosphere–troposphere exchange and middle-atmosphere transport of trace gases. It is shown that the semi-implicit time scheme can be used in a straightforward manner with this discretization. A discussion is given of how to optimize the transition from sigma levels to isentropic levels so as to avoid model levels crossing each other. A numerical problem caused when very shallow, very strong inversions occur in the temperature field is countered by a form of vertical-scale selective dissipation. Baroclinic wave life cycles and full general circulation simulations have been successfully performed with a modified version of the European Centre for Medium-Range Weather Forecasts model.

1. Introduction

There are several potential advantages to be obtained by storing the dependent variables of a numerical general circulation model (GCM) on levels of constant potential temperature. When diabatic heating is small, the potential temperature of an air parcel is approximately conserved so its motion is approximately horizontal with respect to a coordinate frame with potential temperature as the vertical coordinate. In this situation, truncation errors in the model due to vertical advection should be reduced.

In a front, a typical length scale for temperature and wind variations along an isobaric surface may be of the order 100 km, whereas for pressure and wind variations along an isentrope the length scale usually remains at the much larger radius of deformation, that is, of order 1000 km. This, in conjunction with the automatically enhanced vertical resolution due to the close packing of isentropes in a front, makes isentropic coordinates especially suitable for resolving fronts.

These improvements in model performance are accompanied by improvements in the calculation of diagnostics. Less interpolation is required to calculate a quantity like the distribution of potential vorticity (PV) on an isentropic surface, and new and interesting diagnostics such as the accumulated mass flow across an isentropic surface can be more easily calculated.

In practice, previous studies have also revealed several problems with isentropic-coordinate models. Eliassen and Raustein (1968), Bleck (1974), Shapiro (1975), and Trevisan (1976) have used isentropic-coordinate models in which the whole model domain is represented on isentropic levels. Since the ground is not an isentrope, model levels intersect the ground and it is necessary to extrapolate certain fields under the ground in order to calculate horizontal derivatives. This, together with the need to initialize grid points as they emerge above the ground, leads to a certain amount of noise at the surface. It was also anticipated that the formation of superadiabatic layers near the ground might be a problem, causing model levels to overturn or making the height of a model level ambiguous. In fact, these authors reported that such a problem did not occur, although it should be noted that the models they used included no diabatic heating or other boundary-layer parameterizations.

In an attempt to overcome some of these problems, some authors have included a small number of sigma levels (Phillips 1957) close to the ground, typically in the lowest 100 or 200 hPa, with isentropic levels above this region. See, for example, Deavin (1976) (two-dimensional model), Uccellini et al. (1979), Black

* Current affiliation: Department of Meteorology, University of Maryland, College Park, Maryland.

Corresponding author address: Dr. John Thuburn, University of Reading, Department of Meteorology, Reading RG6 2AU, England.

© 1992 American Meteorological Society

Unauthenticated | Downloaded 07/21/24 03:53 AM UTC

(1987), and references therein. Superadiabatic layers can exist in the sigma-coordinate region. Horizontal gradients on isentropes where they intersect the interface can be calculated by interpolating fields where necessary within the sigma-coordinate region. Uccellini et al. (1979) showed how to ensure conservation of mass and energy for transport across the interface. Nevertheless, a certain amount of noise is still generated due to imbalance between the mass and wind fields as new grid points emerge above the interface. Also, some remarks made by Kasahara (1974) still apply: the variable numbers of grid points on the isentropic levels that intersect the interface and the need to interpolate values from sigma levels to isentropic levels mean that the resulting computer code is complicated and is less easy to design to take full advantage of modern computers designed to process arrays efficiently. Furthermore, it would not be practical to implement this technique in a GCM that used a spectral horizontal representation of the model fields.

A third approach is to extend the isentropic model levels horizontally when they reach the ground, resulting in a number of layers of zero or negligible mass at the surface (Bleck 1984; Hsu and Arakawa 1988). This avoids some of the problems mentioned here but introduces new ones. There are discontinuities in various quantities across this extension. For example, the potential vorticity in the massless layers is infinite and representation of this singularity can contaminate other regions of the model. It is also difficult to define a surface temperature.

The continuous primitive equations can be formulated for an arbitrary vertical coordinate, provided that coordinate is monotonic with geometric height (Kasahara 1974). The forecast model of the European Centre for Medium-Range Weather Forecasts (ECMWF) uses a hybrid vertical coordinate that is sigma near the ground and pressure near the top of the model with a smooth transition region in between (Simmons and Burridge 1981). In this paper we describe a technique for incorporating a hybrid vertical coordinate with a smooth transition from sigma levels near the surface to isentropic levels well away from the surface. The technique has been used successfully in the United Kingdom Universities Global Atmospheric Modelling Project (UGAMP) GCM, which is based on the ECMWF cycle 27 forecast model. We hope to obtain, through this technique, some of the potential advantages of using isentropic model levels while avoiding the problems associated with levels intersecting the ground or with matching values at an interface of two domains with different types of model level.

In section 2 details are given of the vertical discretization for a general vertical coordinate in which the model-level pressure is a function of the temperature and surface pressure. In section 3 the particular vertical coordinate used in this study is described and some factors constraining the transitions from one type of model level to another are discussed. In section 4 it is shown that the semi-implicit time scheme can be used with this vertical coordinate with no major modification.

One major problem that can occur in extended integrations is that the pressure difference between two adjacent model half-levels may approach zero and even become negative. In section 5 the circumstances under which this can occur are described in detail, and it is shown that the problem can be cured by including some vertical-scale selective dissipation that acts when model levels become irregularly spaced. Some preliminary results from a GCM integration using the new vertical scheme are shown in section 6.

2. The vertical scheme

The primitive equations for an arbitrary vertical coordinate that is a monotonic function of geometric height are given by Kasahara (1974). Using a notation very similar to that of Simmons and Burridge (1981), the horizontal momentum, thermodynamic energy, mass conservation, and hydrostatic equations may be written:

$$\frac{D\mathbf{v}}{Dt} + f\mathbf{k}\times\mathbf{v} + \nabla\Phi + RT\nabla \ln p = \mathbf{F}, \quad (2.1)$$

$$\frac{DT}{Dt} - \frac{\kappa T\omega}{p} = \frac{Q}{C_p}, \quad (2.2)$$

$$\frac{\partial}{\partial\eta}\left(\frac{\partial p}{\partial t}\right) + \nabla\cdot\left(\mathbf{v}\frac{\partial p}{\partial\eta}\right) + \frac{\partial}{\partial\eta}\left(\dot{\eta}\frac{\partial p}{\partial\eta}\right) = 0 \quad (2.3)$$

$$\frac{\partial\Phi}{\partial\eta} = -\frac{RT}{p}\frac{\partial p}{\partial\eta}. \quad (2.4)$$

Here η is the vertical coordinate, $\mathbf{k}$ is the unit vertical vector, and the other notation is standard. In this coordinate system

$$\frac{D}{Dt} \equiv \frac{\partial}{\partial t} + \mathbf{v}\cdot\nabla + \hat{\omega}\frac{\partial}{\partial p}, \quad (2.5)$$

where $\hat{\omega} = \dot{\eta}\partial p/\partial\eta$ is the vertical velocity relative to the model levels normalized to have the same dimensions as the pressure coordinate vertical velocity, $\omega = Dp/Dt$. By vertically integrating the continuity equation we obtain the following expressions for the ω, the surface pressure tendency, and $\hat{\omega}$:

$$\omega = -\int_0^\eta \nabla\cdot\left(\mathbf{v}\frac{\partial p}{\partial\eta}\right)d\eta + \mathbf{v}\cdot\nabla p, \quad (2.6)$$

$$\frac{\partial p_*}{\partial t} = -\int_0^1 \nabla\cdot\left(\mathbf{v}\frac{\partial p}{\partial\eta}\right)d\eta, \quad (2.7)$$

$$\hat{\omega} = -\frac{\partial p}{\partial t} - \int_0^\eta \nabla\cdot\left(\mathbf{v}\frac{\partial p}{\partial\eta}\right)d\eta. \quad (2.8)$$

Note that an explicit expression for η or $\dot{\eta}$ is not needed. It should also be noted that although both (2.2) and (2.3) appear to be prognostic equations, the time de-

Unauthenticated | Downloaded 07/21/24 03:53 AM UTC

rivative of p is related to the time derivative of T via the coordinate definition. However, these equations may be combined to give a prognostic equation for either p or T (we choose the latter) together with a diagnostic equation for $\hat{\omega}$.

The scheme described by Simmons and Burridge (1981) is easily modified to accommodate θ as well as σ and p levels. It is necessary only to extend the definition of the half-level pressure to allow it to depend on temperature as well as surface pressure:

$$p_{k+1/2} = p_{k+1/2}(p_*, T_{k+1/2}) \quad k = 0, 1, \cdots, N. \quad (2.9)$$

Here N is the number of full levels (so that there are $N+1$ half-levels including the surface, $p_{N+1/2} = p_*$, and the top, $p_{1/2} = 0$). The upper boundary condition $p_{1/2} = 0$ preserves the conservation of angular momentum and energy (Kasahara 1974). The model prognostic variable T is stored on full levels so it is necessary to define the half-level temperatures. The simplest choice (which will be discussed below in section 5) is

$$T_{k+1/2} = \frac{1}{2}(T_k + T_{k+1}). \quad (2.10)$$

Horizontal derivatives of pressure are then given by

$$\nabla p_{k+1/2} = E_{k+1/2}\nabla p_* + \frac{1}{2}F_{k+1/2}(\nabla T_k + \nabla T_{k+1}) \quad (2.11)$$

where

$$E_{k+1/2} = \frac{\partial p_{k+1/2}}{\partial p_*} \quad (2.12)$$

and

$$F_{k+1/2} = \frac{\partial p_{k+1/2}}{\partial T_{k+1/2}}. \quad (2.13)$$

Similarly, the pressure tendencies are

$$\frac{\partial p_{k+1/2}}{\partial t} = E_{k+1/2}\frac{\partial p_*}{\partial t} + \frac{1}{2}F_{k+1/2}\left(\frac{\partial T_k}{\partial t} + \frac{\partial T_{k+1}}{\partial t}\right). \quad (2.14)$$

Defining

$$\Delta p_k = p_{k+1/2} - p_{k-1/2}, \quad (2.15)$$

the finite-difference analogs of (2.7) and (2.8) are

$$\frac{\partial p_*}{\partial t} = -\sum_{r=1}^{N} \nabla\cdot(\mathbf{v}_r \Delta p_r) \quad (2.16)$$

and

$$\hat{\omega}_{k+1/2} = -\frac{\partial p_{k+1/2}}{\partial t} - \sum_{r=1}^{k} \nabla\cdot(\mathbf{v}_r \Delta p_r). \quad (2.17)$$

The finite-difference form

$$\left(\hat{\omega}\frac{\partial \chi}{\partial p}\right)_k = \frac{1}{2\Delta p_k} \times [\hat{\omega}_{k+1/2}(\chi_{k+1} - \chi_k) + \hat{\omega}_{k-1/2}(\chi_k - \chi_{k-1})] \quad (2.18)$$

for the vertical advection of any quantity χ ensures that these terms preserve the conservation of energy and angular momentum.

The temperature tendency obviously depends on the vertical advection of temperature, and (2.8) shows that the vertical advection terms depend on the pressure tendency. A major consequence of allowing the half-level pressure to depend on temperature is that the pressure tendency now depends on the temperature tendency. Nevertheless, it is possible to rearrange equations (2.2), (2.8), and the continuous form of (2.14) to find $\hat{\omega}$ (and hence the temperature and pressure tendencies) in terms of known quantities. To obtain the corresponding finite-difference formula, we first rewrite the thermodynamic equation as

$$\frac{\partial T_k}{\partial t} = \tilde{Q}_k - \frac{1}{2\Delta p_k}[\hat{\omega}_{k+1/2}(T_{k+1} - T_k) + \hat{\omega}_{k-1/2}(T_k - T_{k-1})] \quad (2.19)$$

where $\tilde{Q}$ is the contribution to the temperature tendency from all processes except vertical advection. A diagnostic equation for $\hat{\omega}$ may be obtained by demanding that this temperature tendency is consistent with the pressure tendency given by the continuity equation. Combining (2.19) with (2.14) and (2.17) gives

$$\mathbf{H}\hat{\omega} = \mathbf{R} \quad (2.20)$$

where

$$\hat{\omega} = (\hat{\omega}_{3/2}, \hat{\omega}_{5/2}, \cdots, \hat{\omega}_{N-1/2})^{\mathrm{T}}, \quad (2.21)$$

$$\mathbf{R} = (R_{3/2}, R_{5/2}, \cdots, R_{N-1/2})^{\mathrm{T}}, \quad (2.22)$$

$$R_{k+1/2} = -E_{k+1/2}\frac{\partial p_*}{\partial t} - \sum_{r=1}^{k} \nabla\cdot(\mathbf{v}_r \Delta p_r) - \frac{1}{2}F_{k+1/2}(\tilde{Q}_k + \tilde{Q}_{k+1}), \quad (2.23)$$

and $\mathbf{H}$ is a tridiagonal matrix

$$\left.\begin{aligned} H_{k,k} &= 1 - \frac{1}{4}F_{k+1/2}\left(\frac{1}{\Delta p_k} + \frac{1}{\Delta p_{k+1}}\right) \times (T_{k+1} - T_k), \\ H_{k,k-1} &= -\frac{1}{4\Delta p_k}F_{k+1/2}(T_k - T_{k-1}), \\ H_{k,k+1} &= -\frac{1}{4\Delta p_{k+1}}F_{k+1/2}(T_{k+2} - T_{k+1}), \\ H_{i,j} &= 0 \quad \text{otherwise.} \end{aligned}\right\} \quad (2.24)$$

At each horizontal grid point the linear system (2.24) can be solved efficiently using a variation of the Gaussian elimination method. For sigma, pressure, or hybrid sigma–pressure levels $F_{k+1/2} = 0$ and $\mathbf{H}$ reduces to the identity matrix.

Unauthenticated | Downloaded 07/21/24 03:53 AM UTC

Note that it is necessary to calculate $\tilde{Q}$ before we can determine $\hat{\omega}$. That is, we must calculate the contributions from all the physical parameterizations before the adiabatic part of the time step can be completed.

The finite-difference expressions for the geopotential,

$$\Phi_k = \Phi_* + \sum_{r=k+1}^{N} RT_r \ln\left(\frac{p_{k+1/2}}{p_{k-1/2}}\right) + \alpha_k RT_k, \quad (2.25)$$

the pressure gradient term,

$$(RT\nabla \ln p)_k = \frac{RT_k}{\Delta p_k}\left[\ln\left(\frac{p_{k+1/2}}{p_{k-1/2}}\right)\nabla p_{k-1/2} + \alpha_k \nabla(\Delta p_k)\right], \quad (2.26)$$

and the energy conversion term,

$$\left(\frac{\kappa T\omega}{p}\right)_k = \frac{\kappa T_k}{\Delta p_k} \times \left\{-\left[\ln\left(\frac{p_{k+1/2}}{p_{k-1/2}}\right)\sum_{r=1}^{k-1} \nabla\cdot(\mathbf{v}_r \Delta p_r) + \alpha_k \nabla\cdot(\mathbf{v}_k \Delta p_k)\right] + \mathbf{v}_k\cdot\left[\ln\left(\frac{p_{k+1/2}}{p_{k-1/2}}\right)\nabla p_{k-1/2} + \alpha_k \nabla(\Delta p_k)\right]\right\}, \quad (2.27)$$

take the general forms given by Simmons and Burridge (1981), who showed that they preserve the angular momentum and energy conservation properties.[1] In tests of the method the following values of α_k have been used:

$$\alpha_k = 1 - \frac{p_{k-1/2}}{\Delta p_k}\ln\left(\frac{p_{k+1/2}}{p_{k-1/2}}\right), \quad k = 2, \cdots, N, \quad (2.28)$$

with either $\alpha_1 = \ln 2$ or $\alpha_1 = 1$.

3. The model levels

As remarked in section 2, an explicit expression for the vertical coordinate η is not needed, but we do need to define the half-level pressure in terms of the temperature and surface pressure. A convenient definition is

$$d_{k+1/2}p_{k+1/2} = a_{k+1/2} + b_{k+1/2}p_* - c_{k+1/2}p_{k+1/2}T_{k+1/2}^{-1/\kappa}. \quad (3.1)$$

Four constants, a, b, c, and d, define each model half-level, and this set of constants may be referred to as the vertical coordinate table. If both b and c are zero the pressure is constant on the half-level; if a and c are zero it is a sigma half-level; and if b and d are zero it is an isentropic half-level. By a suitable choice of these constants a smooth transition can be made between σ, θ, and p levels. The hybrid σ–p coordinate used in the ECMWF forecast model is a special case, with c zero and d unity, of this more general coordinate.

The explicit forms for E and F are

$$E_{k+1/2} = \frac{b_{k+1/2}}{(d_{k+1/2} + c_{k+1/2}T_{k+1/2}^{-1/\kappa})}, \quad (3.2)$$

$$F_{k+1/2} = \frac{c_{k+1/2}p_{k+1/2}T_{k+1/2}^{-1/\kappa}}{\kappa T_{k+1/2}(d_{k+1/2} + c_{k+1/2}T_{k+1/2}^{-1/\kappa})}. \quad (3.3)$$

The choice of the vertical coordinate table is determined within the following general constraints:

(i) At least one half-level of constant sigma at the surface follows the terrain.

(ii) It may also be desirable to have one or more half-levels of constant pressure at the top where model levels are widely spaced in height; otherwise truncation errors can lead to poor cancellation in the pressure gradient term, $\nabla\Phi + RT\nabla \ln p$, giving rise to large wind errors.

(iii) There should be smooth transitions from sigma levels to isentropic levels, and from isentropic levels to pressure levels, so that the model is well behaved. In particular, model levels should not cross each other.

(iv) Subject to (i), (ii), and (iii), it is desirable for as many model levels as possible to be isentropic surfaces.

The same model level is defined by (3.1) when a, b, c, and d are multiplied by a constant factor. This redundancy can be used to satisfy one further constraint:

(v) $a_{k+1/2} + b_{k+1/2}p_*$ should approximately give the pressure on half-level $k + 1/2$. Equivalently, $d_{k+1/2} + c_{k+1/2}T_{k+1/2}^{-1/\kappa}$ should approximately equal 1. This ensures that a reasonable reference pressure profile is used in the semi-implicit time scheme—see section 4.

In the Appendix a convenient method is described for choosing the vertical coordinate table consistent with these constraints.

Some idealized baroclinic instability life-cycle experiments have been performed without orography and without parameterizations of physical processes. In this case the transition from sigma levels to isentropic levels can be made quite rapidly; an example vertical coordinate table is Table A1 in the Appendix. When the model is run with realistic orography and physical parameterizations switched on the transition to isentropic levels is limited by high orography. For example, in the Northern Hemisphere summer the Himalayan region can have a surface potential temperature of 335 K, so the transition to isentropic surfaces cannot occur below this level. The vertical coordinate in Table A2 of the Appendix has been successfully used in some full GCM experiments. It gives a lowest pure isentropic full level at about 352 K. For both of these sample

[1] For a model that uses a spectral representation of T and $\ln p_*$ in the horizontal, because $\nabla p_{k+1/2}$ is evaluated using (2.11) with $\nabla p_* = p_*\nabla \ln p_*$, there is no formal guarantee that the discrete analog of $\int_0^{2\pi} d\lambda \partial p_{k+1/2}/\partial\lambda = 0$ holds, so the horizontal discretization does not formally conserve angular momentum. This is true even for a hybrid sigma–pressure-coordinate model. In practice, however, the errors are very small.

Unauthenticated | Downloaded 07/21/24 03:53 AM UTC

vertical coordinate tables the transition from isentropic levels to pressure levels is made rapidly over the top 3 half levels. Figure 1 shows the zonal mean locations of the full model levels at the start of an integration using the hybrid σ–θ–p coordinate as in Table A2.

4. Semi-implicit time scheme

Following the pioneering study of the semi-implicit method by Robert et al. (1972), Bourke (1974) and Hoskins and Simmons (1975) showed how stable integrations of a spectral model can be achieved with relatively long time steps by calculating some of the gravity-wave contributions to the divergence, temperature, and surface pressure increments implicitly.

The equations for divergence, temperature, and surface pressure, linearized about an isothermal ($T = T_{\text{ref}}$) state of rest and a particular reference pressure profile $p_{\text{ref}}(\eta)$, are

$$\frac{\partial D}{\partial t} - \int_0^\eta \frac{R\nabla^2 T'}{p_{\text{ref}}} \frac{\partial p_{\text{ref}}}{\partial \eta}\, d\eta + \frac{RT_{\text{ref}}}{p_{*\text{ref}}} \nabla^2 p'_* = 0, \quad (4.1)$$

$$\frac{\partial T'}{\partial t} + \frac{\kappa T_{\text{ref}}}{p_{\text{ref}}} \int_0^\eta D \frac{\partial p_{\text{ref}}}{\partial \eta}\, d\eta = 0, \quad (4.2)$$

$$\frac{\partial p'_*}{\partial t} = -\int_0^1 D \frac{\partial p_{\text{ref}}}{\partial \eta}\, d\eta, \quad (4.3)$$

where $T' = T - T_{\text{ref}}$ and $p'_* = p_* - p_{*\text{ref}}$ and we have substituted expressions for ω and for the geopotential perturbation Φ'. It is clear from (4.1)–(4.3) that p'_* and the vertical structure of D and T' for linear gravity waves depend only on $\partial p_{\text{ref}}/\partial \eta$ and are otherwise independent of the type of vertical coordinate. (However, the vertical structure of p' and Φ' do depend on the type of vertical coordinate.) This implies that, for gravity-wave terms determined with respect to an isothermal reference state, the corrections to the divergence, temperature, and surface pressure equations should be independent of the type of vertical coordinate. This can be verified for the hybrid sigma–pressure coordinate of Simmons and Burridge (1981) by substituting a constant reference temperature into the expressions given in their Appendix.

Following the ECMWF practice, the UGAMP GCM uses an isothermal reference profile in its semi-implicit scheme so the scheme does not need to be modified to use the more general coordinate. The reference temperature chosen is 300 K, rather warmer than a typical temperature in the model atmosphere. The work of Simmons et al. (1978) shows that this improves the stability properties of the semi-implicit scheme.

Simmons and Burridge (1981) define their reference pressure profile by specifying $p_{*\text{ref}} = 800$ hPa and substituting this into their definition of half-level pressures: $p_{k+\frac{1}{2}\text{ref}} = A_{k+\frac{1}{2}} + B_{k+\frac{1}{2}} p_{*\text{ref}}$. If we attempt to define a reference pressure profile by substituting $p_{*\text{ref}} = 800$ hPa and $T_{\text{ref}} = 300$ K into (3.1) absurd values of $p_{k+\frac{1}{2}\text{ref}}$ can be obtained (because the reference temperature is so warm) and the resulting semi-implicit scheme is highly unstable. Provided $a_{k+\frac{1}{2}}$ and $b_{k+\frac{1}{2}}$ have been suitably chosen as in section 3 point (v), we can define the reference-pressure profile by $p_{k+\frac{1}{2}\text{ref}} = a_{k+\frac{1}{2}} + b_{k+\frac{1}{2}} p_{*\text{ref}}$ (with $p_{*\text{ref}} = 800$ hPa). The resulting semi-implicit scheme performs well in practice.

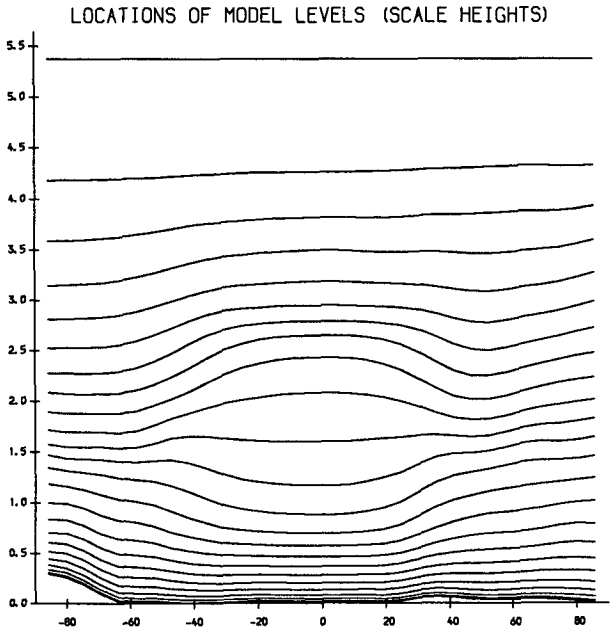

FIG. 1. Zonal mean locations of model levels in scale heights $[-\ln(p/p_0)$, where $p_0 = 10^5$ Pa], for the initial state of an integration beginning on 15 January. The levels are defined using vertical coordinate Table A2 in the Appendix. The lowest pure isentropic level is the 11th level from the top at 352 K.

5. The problem of levels crossing and a solution

If at any point $p_{k-\frac{1}{2}}$ becomes greater than $p_{k+\frac{1}{2}}$, that is, the model half-levels cross each other, the numerical solution rapidly "blows up." There are two circumstances under which this can occur. The first is when the vertical coordinate table is badly chosen with the transition from one type of vertical coordinate to another occurring too rapidly. An explanation of how to choose the vertical-coordinate table to avoid this problem is given in the Appendix.

The second circumstance is when a very thin, very stably stratified layer forms in the region of isentropic levels. This happened, for example, in an extended "perpetual January" simulation using the UGAMP GCM at around 200 hPa over Antarctica where a sharp fall in the concentration of water vapor with height led to a strong peak in the radiative cooling at one model level. In one experiment the model levels crossed after about 70 days of the integration. If such a structure is realistic, it is clear that it is not resolved adequately by the vertical discretization. Here the numerical problem posed by the possibility of levels crossing is examined.

Unauthenticated | Downloaded 07/21/24 03:53 AM UTC

The pressure on an isentropic half-level is

$$p_{k+1/2} = p_0\left(\frac{T_{k+1/2}}{\theta_{k+1/2}}\right)^{1/\kappa}, \tag{5.1}$$

($p_0 = 10^5$ hPa), where $\theta_{k+1/2}$ is fixed for each isentropic level. If $T_{k+1/2}$ decreases then $p_{k+1/2}$ decreases, and this level moves up. If $T_{k+1/2}$ increases $p_{k+1/2}$ increases, and this level moves down. If level $k + 1/2$ cools sufficiently relative to level $k - 1/2$ the levels will eventually meet when

$$p_{k+1/2} = p_{k-1/2}, \tag{5.2}$$

that is, when

$$\frac{T_{k-1/2}}{T_{k+1/2}} = \frac{\theta_{k-1/2}}{\theta_{k+1/2}}. \tag{5.3}$$

At first it seems unphysical and counterintuitive that half-level $k - 1/2$ can continue to warm relative to half-level $k + 1/2$ even when they become very close. To explain this we must look more closely at the vertical discretization.

Pressure on model half-levels is a fundamental quantity of the model discretization, whereas the full-level pressure is a secondary quantity. The half-level pressure $p_{k+1/2}$ is defined in terms of the vertical coordinate table, the surface pressure p_* and the half-level temperature $T_{k+1/2}$, while p_k is given simply by

$$p_k = \frac{1}{2}(p_{k-1/2} + p_{k+1/2}). \tag{5.4}$$

The converse is true for temperature: full-level temperature T_k is a model prognostic variable while the half-level temperature is defined by

$$T_{k+1/2} = \frac{1}{2}(T_k + T_{k+1}). \tag{5.5}$$

Here $T_{k+1/2}$ is used only in calculating the half-level pressure. Figure 2 shows a typical distribution of levels when levels $k + 1/2$ and $k - 1/2$ are close to crossing but all other levels are well spaced. Half-level $k - 1/2$ warms relative to half-level $k + 1/2$ because level $k - 1$ warms relative to level $k + 1$. Levels $k - 1$ and $k + 1$ can have significantly different diabatic heating rates because they remain a finite distance apart and so can retain distinct properties, such as moisture mixing ratio, even as the half-levels $k - 1/2$ and $k + 1/2$ approach each other.

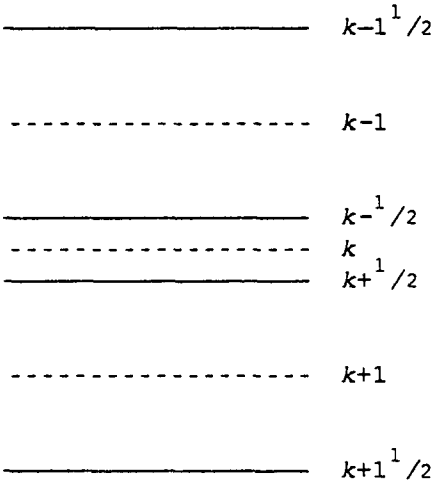

FIG. 2. Typical distribution of model levels in pressure space when levels $k - 1/2$ and $k + 1/2$ are close to crossing. Dashed lines represent full levels, solid lines represent half-levels.

An approximate condition for levels to cross can be expressed in terms of the vertical temperature gradient. Defining $T_{k+1/2} - T_{k-1/2} = \Delta T_k$ and $\theta_{k+1/2} - \theta_{k-1/2} = \Delta\theta_k$, levels meet when

$$\Delta T_k = \left(\frac{p_k}{p_0}\right)^{\kappa}\Delta\theta_k. \tag{5.6}$$

The temperature gradient that would be diagnosed from the model state is

$$\left(\frac{\partial T}{\partial z}\right)_k = \frac{T_{k+1} - T_{k-1}}{z_{k+1} - z_{k-1}}. \tag{5.7}$$

Because the full levels are still fairly evenly spaced we assume $z_{k+1} - z_{k-1} \approx 2(\Delta z)_0$, where $(\Delta z)_0$ is a typical level spacing in the absence of strong vertical temperature gradients. Then, substituting from (5.6),

$$\left(\frac{\partial T}{\partial z}\right)_k \approx \frac{2\Delta T_k}{2(\Delta z)_0} \approx \left(\frac{p_k}{p_0}\right)^{k}\frac{\Delta\theta_k}{(\Delta z)_0}. \tag{5.8}$$

For an isothermal atmosphere $(p/p_0)^k\partial\theta/\partial z = g/c_p$ so the criterion for levels to meet is

$$\left(\frac{\partial T}{\partial z}\right)_k \approx \frac{g}{c_p} \approx 9.8\ \text{K km}^{-1}. \tag{5.9}$$

An inversion as strong as this is seen in the model just before the levels cross.

The criterion (5.9) applies only when the strong inversion covers only two levels, as depicted in Fig. 2. The calculation can be repeated assuming the inversion extends over more levels. In this case, however, the restriction is less severe than (5.9).

Equation (5.9) gives a limit to the strength of an inversion on the scale of the model grid that can be represented in this hybrid-coordinate model in the region of pure isentropic levels. (To be more precise, it is the close juxtaposition of strong inversion and more usual stratification that cannot be represented.) The main reason for this limitation can be traced back to equation (5.5) for the half-level temperature, which is obviously inappropriate in a situation like that shown in Fig. 2.

Since the problem is caused by the presence of features in the temperature profile with small vertical scale that are poorly resolved, the most natural solution is to increase the vertical resolution in the region of interest. The calculation described above shows that

Unauthenticated | Downloaded 07/21/24 03:53 AM UTC

model levels will not cross provided (the edge of) the inversion is adequately resolved. However, it is not always convenient to increase a model's resolution, nor it is obvious what resolution is likely to be needed.

This argument suggests that an alternative expression for the half-level temperature might cure the problem. For example, $T_{k+1/2}$ could be obtained by interpolating linearly in p between levels k and $k+1$. However, we need to know the half-level T before we can calculate p (either half-level or full level). Furthermore, for any expression of the form

$$T_{k+1/2} = \gamma_1 T_k + \gamma_2 T_{k+1}, \tag{5.10}$$

the tendencies and horizontal gradients of γ_1 and γ_2 need to be taken into account in calculating the tendencies and horizontal gradients of p. These facts mean that the dynamical calculations would be extremely impractical, if not impossible, for anything other than constant γ_1 and γ_2.

An alternative approach is to recognize that the vertical discretization is not designed for situations where the layer thickness Δp_k varies greatly from one layer to the next. Since the finite differences will be inaccurate, such circumstances should not be allowed to arise. A situation like that in Fig. 2 could occur if the diabatic heating increases sharply between level $k+1$ and level $k-1$. This occurred in the case of levels crossing as previously described and, indeed, the parameterization schemes in this version of the UGAMP GCM can give rise to rather noisy profiles of heating above about 200 hPa at all latitudes. Ideally, parameterization schemes should be developed that give less noisy heating profiles. As an interim measure, smoothing the profile of diabatic heating might be one way to prevent levels crossing. We have chosen, instead, to smooth any sharp changes in the vertical gradient of temperature by artificially enhancing the vertical diffusion in these regions. This is not intended to represent any physical mechanism operating in the real atmosphere. On the contrary, vertical mixing is expected to be a minimum in strongly stably stratified regions. This technique should be regarded purely as a numerical artifice to prevent any grid-scale inversions from becoming stronger than can be represented accurately by the grid and finite-difference scheme.

In one example, shown in section 6, the UGAMP GCM includes a vertical diffusion parameterization in which the diffusion coefficients K_m (acting on momentum) and K_h (acting on dry static energy and moisture) depend on the Richardson number, the vertical shear, and a mixing length. We replace K_m by $\beta\tilde{K}_m + (1-\beta)K_m$ where $\tilde{K}_m$ has a large fixed value; K_h is treated similarly. The half-level values of β are defined by

$$\beta_{k+1/2} = \max\left\{1.0, \frac{\Delta p_{k+1} + \Delta p_k + \Delta p_{k-1}}{6\Delta p_k}, \frac{\Delta p_{k+2} + \Delta p_{k+1} + \Delta p_k}{6\Delta p_{k+1}}\right\} - 1.0. \tag{5.11}$$

We can see from Fig. 3 that the enhanced diffusion switches on when the ratio of adjacent layer thicknesses exceeds about 2.5 and rapidly increases as this ratio increases. The values chosen for $\tilde{K}_m$ and $\tilde{K}_h$ are

$$\left.\begin{aligned}\tilde{K}_m &= 25\ \text{m}^2\ \text{s}^{-1},\\ \tilde{K}_h &= 187.5\ \text{m}^2\ \text{s}^{-1}.\end{aligned}\right\} \tag{5.12}$$

(Without this enhancement values of K_m and K_h in the model vary greatly but are typically of the order 1–10 $\text{m}^2\ \text{s}^{-1}$.) We expect the model behavior to be insensitive to the exact values used, so long as they are large. The effective limit to the inversion strength will depend on the exact shape of the curve shown in Fig. 3. In the boundary layer of the model the ratio of adjacent layer thicknesses can be almost as large as 2.5, so if we wish to use a similar distribution of levels we should not switch on the enhanced diffusion for ratios smaller than this.

In practice, the enhanced diffusion acts occasionally and in local regions, switching on and off smoothly over a number of time steps with small values of β, typically of the order 10^{-2}. The "perpetual January" simulation described previously was rerun successfully for 200 days with this enhanced vertical diffusion and, indeed, the vertical profile of temperature is noticeably less noisy above 200 hPa.

The use of horizontal-scale selective dissipation in GCMs is a well-established and accepted technique for smoothing features in model fields that would otherwise have too small a horizontal length scale to be resolved properly. The enhanced diffusion described above can be interpreted as a vertical-scale selective dissipation that smooths features that would otherwise have too small a vertical length scale to be resolved properly.

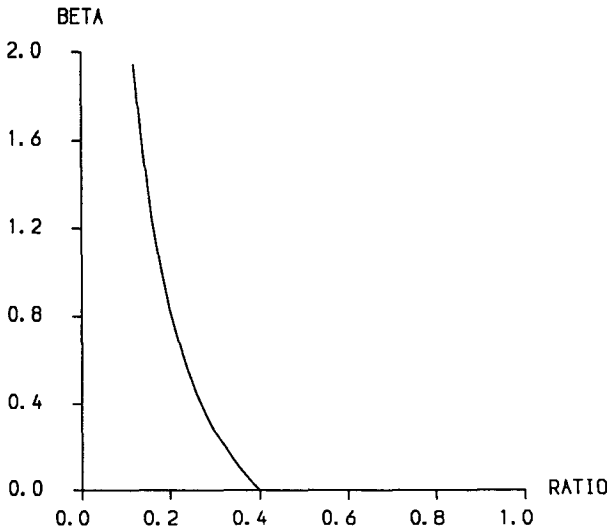

FIG. 3. The diffusion enhancement factor $\beta_{k+1/2}$ defined by (5.11), as a function of $\Delta p_k/(\Delta p)_0$ assuming $\Delta p_{k+1} = \Delta p_{k-1} = (\Delta p)_0$.

Unauthenticated | Downloaded 07/21/24 03:53 AM UTC

6. Preliminary results

The hybrid isentropic coordinate vertical scheme was first tested by performing some idealized baroclinic instability life-cycle experiments at T42 horizontal resolution using the 15 levels defined in Table A1. All physical parameterizations were switched off in an attempt to isolate the effects of the new vertical coordinate. In particular, the enhanced vertical diffusion described in section 5 was not used in these experiments. The results are rather encouraging, with some evidence that potential vorticity is slightly better conserved following air parcels when hybrid isentropic model levels are used, when compared with a corresponding sigma coordinate experiment. On the other hand, the final zonal wind and temperature distributions are almost identical in the two experiments.

The new vertical scheme has also been tested in some general circulation simulations, including parameterizations of radiation, convection, condensation, vertical mixing, gravity-wave drag, and surface processes. For example, Fig. 4 shows the zonal-mean zonal wind and temperature, time averaged from day 330 to day 360, from an annual cycle experiment beginning on 15 January using T21 horizontal resolution and 24 levels defined in Table A2. The lowest pure isentropic full level is at approximately 352 K. The rate of transition from sigma levels to isentropic levels is limited in this case by the height of the orography and the relative warmth of the Tibetan Plateau during the northern summer. Figure 5 shows the same fields as Fig. 4 from a corresponding sigma–pressure-coordinate simulation with levels defined by the a's and b's in Table A2. It appears, from simple diagnostics such as these, that models with the two types of vertical coordinate produce broadly similar climates. There is some suggestion that the temperature field around the tropopause and in the

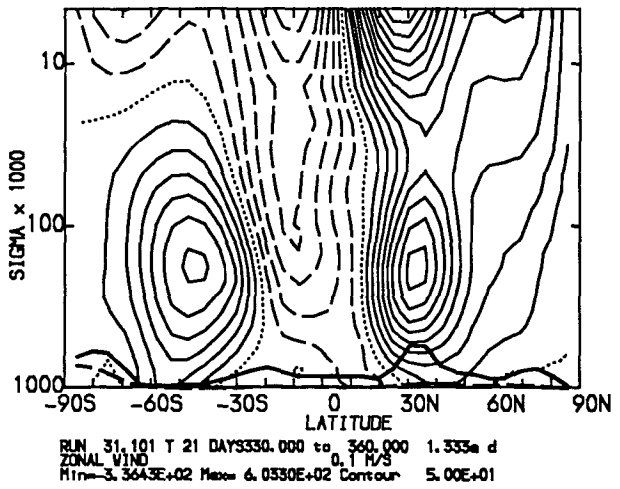

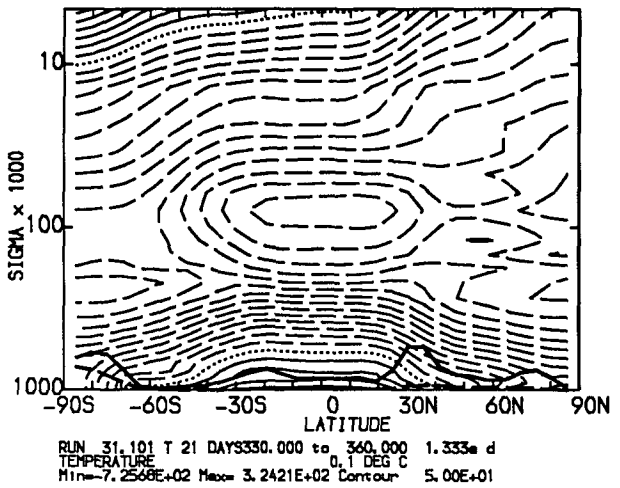

FIG. 4. The zonal-mean zonal wind (contour 5 m s^{-1}) and zonal mean temperature (contour 5°C) averaged from day 330 to day 360 from an integration using the hybrid isentropic coordinate. Negative contours are dashed and the zero contour is dotted.

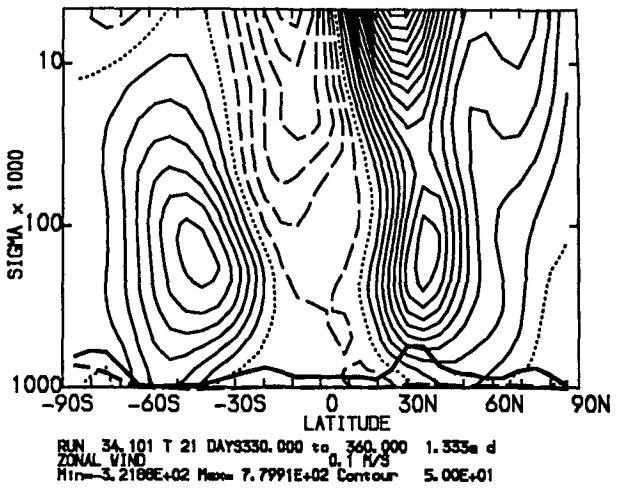

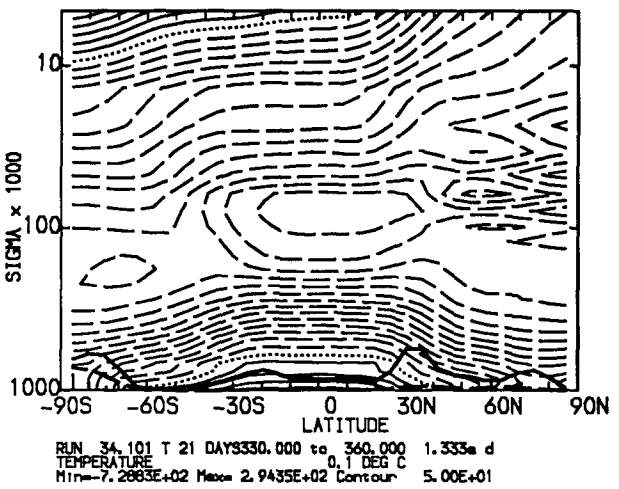

FIG. 5. As in Fig. 4 except from an integration using a sigma–pressure vertical coordinate.

Unauthenticated | Downloaded 07/21/24 03:53 AM UTC

winter stratosphere is less noisy in the hybrid isentropic-coordinate simulation. This is probably due to the enhanced vertical diffusion compensating for some model errors by acting directly on the temperature field and also by acting on the moisture field, which results in a smoother profile of radiative heating. Detailed diagnostics from the baroclinic instability experiments and from the general circulation simulations will be presented elsewhere.

7. Discussion and conclusions

In this paper we have shown how to extend the energy- and angular momentum–conserving scheme of Simmons and Burridge (1981) to use a hybrid coordinate that changes smoothly from sigma levels near the ground to isentropic levels higher up. In either pressure coordinates or sigma coordinates, the continuity equation is a diagnostic equation for ω, whereas the thermodynamic equation may be written as a prognostic equation for θ. In isentropic coordinates the roles are reversed. In purely isentropic coordinate models, one usually writes the thermodynamic equation as a diagnostic equation for the vertical velocity $\dot{\theta}$ while the model-level pressure is predicted using the tendency given by the continuity equation. In order to accommodate this exchange of roles in the transition from sigma levels to isentropic levels, we have chosen to retain the thermodynamic equation as a prognostic equation for the temperature T. The thermodynamic and continuity equations must be combined, along with the definition of the model levels, in order to diagnose the vertical velocity $\hat{\omega}$ (with the vertical discretization described here this requires a tridiagonal linear system to be solved), and hence to obtain the temperature tendency in terms of known quantities. In regions of sigma–pressure levels the scheme reduces to that of Simmons and Burridge (1981). In regions of isentropic levels the scheme differs slightly from the more usual isentropic-coordinate model formulations in that temperature is predicted and then model-level pressure is diagnosed, rather than pressure predicted and temperature diagnosed. In isentropic or hybrid isentropic coordinates the vertical advection terms depend on the heating rate $\dot{\theta}$ so contributions to $\dot{\theta}$ from parameterized physical processes must be calculated before the vertical advection terms.

Integrations of a GCM incorporating this hybrid σ–θ–p vertical coordinate have been performed successfully. These include idealized baroclinic instability life-cycle experiments and integrations with realistic orography and a number of parameterized physical processes.

Acknowledgments. This work was carried out as part of the UGAMP project funded by the United Kingdom Natural Environment Research Council. The authors are grateful to Dr. A. J. Simmons for some helpful discussions.

APPENDIX

Choosing the Vertical-Coordinate Table

In this appendix a convenient algorithm for choosing the vertical-coordinate table is described and the factors that limit the transition from sigma levels to isentropic levels are discussed.

First, choose values of sigma ($\hat{\sigma}_{k+1/2}$, say) that will approximately describe the positions of the model half levels. Also estimate the values of temperature or potential temperatures at these levels ($\hat{T}_{k+1/2} = \hat{\sigma}^{\kappa}_{k+1/2}\hat{\theta}_{k+1/2}$, say). For a sigma level

$$a_{k+1/2} = 0, \quad b_{k+1/2} = \hat{\sigma}_{k+1/2}, \quad c_{k+1/2} = 0, \quad d_{k+1/2} = 1. \tag{A.1}$$

For a pressure level

$$a_{k+1/2} = \hat{\sigma}_{k+1/2}p_0, \quad b_{k+1/2} = 0, \quad c_{k+1/2} = 0, \quad d_{k+1/2} = 1. \tag{A.2}$$

For an isentropic level

$$a_{k+1/2} = \hat{\sigma}_{k+1/2}p_0, \quad b_{k+1/2} = 0, \quad c_{k+1/2} = \hat{T}^{1/\kappa}_{k+1/2}, \quad d_{k+1/2} = 0. \tag{A.3}$$

We also need to choose values of a, b, c, and d in the transition levels. A convenient way to do this is to parameterize the transition from sigma levels to isentropic levels by some parameter, λ, say. Thus, $\lambda_{k+1/2} = 0$ for sigma levels and $\lambda_{k+1/2} = 1$ for isentropic levels (and in the transition to pressure levels); λ takes values between 0 and 1 in the transition levels. Similarly, we parameterize the transition to pressure levels at the top by another parameter, μ; $\mu_{k+1/2} = 1$ for sigma or isentropic levels, and $\mu_{k+1/2} = 0$ for pressure levels. A general formula for the constants in the vertical-coordinate table is then

$$\left.\begin{aligned} a_{k+1/2} &= \lambda_{k+1/2}\hat{\sigma}_{k+1/2}p_0, \\ b_{k+1/2} &= (1 - \lambda_{k+1/2})\hat{\sigma}_{k+1/2}, \\ c_{k+1/2} &= \lambda_{k+1/2}\mu_{k+1/2}\hat{T}^{1/\kappa}_{k+1/2}, \\ d_{k+1/2} &= (1 - \lambda_{k+1/2}\mu_{k+1/2}). \end{aligned}\right\} \tag{A.4}$$

We need to choose values of λ and μ for the transition levels. An example vertical-coordinate table is shown in Table A1. The values of λ and μ were chosen mainly by guesswork. This vertical-coordinate table, which has a lowest isentropic full level at approximately 315 K, has been used in some idealized baroclinic instability life-cycle experiment with no orography and no parameterized physical processes.

In fact, it is possible to make some analytical estimates of the maximum rate of transition subject to the condition that levels do not cross. We will consider the transition from sigma levels to isentropic levels and so set $\mu = 0$ in (A.4). We will also omit the subscripts $k + 1/2$ and regard λ, $\hat{T}$, T, and p as continuous functions of $\hat{\sigma}$. The problem is then: How large can we make $-d\lambda/d\ln\hat{\sigma}$ without $dp/d\hat{\sigma}$ becoming negative?

Unauthenticated | Downloaded 07/21/24 03:53 AM UTC

TABLE A1. Vertical-coordinate table used in some idealized baroclinic instability life-cycle experiments. The values of $\hat{\sigma}$ were taken from an otherwise identical sigma-coordinate model against which the isentropic coordinate model was compared.

Level	$\hat{\sigma}$	$\hat{\theta}$	λ	μ	$a/10^5$	b	$c/10^9$	d
1/2	0.0	—	1.0	0.0	0.0	0.0	0.0	1.0
1 1/2	0.0369	535	1.0	0.0	0.0369	0.0	0.0	1.0
2 1/2	0.0822	415	1.0	0.5	0.0822	0.0	0.0609	0.5
3 1/2	0.1292	370	1.0	1.0	0.1292	0.0	0.1279	0.0
4 1/2	0.1748	345	1.0	1.0	0.1748	0.0	0.1355	0.0
5 1/2	0.2187	335	1.0	1.0	0.2187	0.0	0.1529	0.0
6 1/2	0.2628	325	1.0	1.0	0.2628	0.0	0.1652	0.0
7 1/2	0.3103	320	1.0	1.0	0.3103	0.0	0.1848	0.0
8 1/2	0.3660	310	1.0	1.0	0.3660	0.0	0.1950	0.0
9 1/2	0.4344	300	0.85	1.0	0.3692	0.0652	0.1754	0.15
10 1/2	0.5187	295	0.70	1.0	0.3631	0.1556	0.1625	0.3
11 1/2	0.6187	290	0.55	1.0	0.3403	0.2784	0.1413	0.45
12 1/2	0.7293	287	0.40	1.0	0.2917	0.4376	0.1168	0.6
13 1/2	0.8395	284	0.25	1.0	0.2099	0.6296	0.0810	0.75
14 1/2	0.9346	282	0.10	1.0	0.0935	0.8411	0.0352	0.9
15 1/2	1.0	—	0.0	1.0	0.0	1.0	0.0	1.0

Substituting (A.4) into (3.1) with $\mu = 1$ gives

$$p = \frac{\hat{\sigma}[\lambda p_0 + (1-\lambda)p_*]}{(1-\lambda) + \lambda(\hat{T}/T)^{1/\kappa}}. \tag{A.5}$$

The marginal case is when $dp/d\hat{\sigma} = 0$, that is,

$$[(1-\lambda) + \lambda(\hat{T}/T)^{1/\kappa}][\lambda p_0 + (1-\lambda)p_* + \hat{\sigma}(p_0 - p_*)d\lambda/d\hat{\sigma}] - \hat{\sigma}[\lambda p_0 + (1-\lambda)p_*] \times \{[(\hat{T}/T)^{1/\kappa} - 1]d\lambda/d\hat{\sigma} + \lambda d(\hat{T}/T)^{1/\kappa}/d\hat{\sigma}\} = 0. \tag{A.6}$$

For the sake of notation we define the following quantities:

$$F = (\hat{T}/T)^{1/\kappa} - 1,$$
$$G = \lambda F + 1,$$
$$H = \lambda p_0 + (1-\lambda)p_*, \tag{A.7}$$

whereupon (A.6) becomes

$$\frac{d\lambda}{d\ln\hat{\sigma}}\left[\frac{G(p_0 - p_*)}{H} - F\right] = \lambda\frac{d(\hat{T}/T)^{1/\kappa}}{d\ln\hat{\sigma}} - G. \tag{A.8}$$

Now consider the term $d(\hat{T}/T)^{1/\kappa}/d\ln\hat{\sigma}$. The largest values of $\hat{T}/T$ are likely to be found at the surface ($\hat{\sigma} = 1, \lambda = 0$) over high orography where the mountaintop T is significantly less than the global estimated surface $\hat{T}$. Higher up, by the time we reach $\lambda = 1$, T should be rather close to $\hat{T}$. Hence, it is better to regard $d(\hat{T}/T)^{1/\kappa}/d\lambda$ as the known quantity and use

$$\frac{d(\hat{T}/T)^{1/\kappa}}{d\ln\hat{\sigma}} = \frac{d(\hat{T}/T)^{1/\kappa}}{d\lambda}\frac{d\lambda}{d\ln\hat{\sigma}}. \tag{A.9}$$

Then (A.8) becomes

$$-\frac{d\lambda}{d\ln\hat{\sigma}} = \left[\frac{(p_0 - p_*)}{H} - \frac{F}{G} - \frac{\lambda}{G}\frac{d(\hat{T}/T)^{1/\kappa}}{d\lambda}\right]^{-1}. \tag{A.10}$$

The most stringent conditions are provided by the minimum value of the right-hand side of (A.10). Thus, the conditions that permit only a slow rate of transition are:

(a) small p_* (high orography),
(b) small H, (small p_* and small λ),
(c) F negative, (T is greater than the estimate $\hat{T}$),
(d) small G, provided (c) holds (this is consistent),
(e) $d(\hat{T}/T)^{1/\kappa}/d\lambda$ negative and λ close to 1,
(f) small G, provided (e) holds.

Obviously, not all of these conditions will hold at the same time.

We can estimate some typical values for the quantities in (A.10) applicable to a GCM with envelope orography:

$$-0.3 \leqslant F \leqslant 0.5, \tag{A.11}$$

$$\left.\begin{aligned} &G = 1, \quad \lambda = 0, \\ &0.7 \leqslant G \leqslant 1.5, \quad \lambda = 1, \end{aligned}\right\} \tag{A.12}$$

$$\left.\begin{aligned} &0.45p_0 \leqslant H \leqslant p_0, \quad \lambda = 0, \\ &H = p_0, \quad \lambda = 1. \end{aligned}\right\} \tag{A.13}$$

Over high orography where, perhaps, $T \approx 230$ K but $\hat{T} = 280$ K at the surface and $T \approx \hat{T}$ higher up above the transition to θ levels,

$$\frac{\Delta(\hat{T}/T)^{1/\kappa}}{\Delta\lambda} \approx -1. \tag{A.14}$$

Hence, we can estimate the marginal transition rate:

(i) At $\lambda = 0$ the orography term dominates the temperature term (indeed, F will usually be positive at mountaintops)

$$-\frac{d\lambda}{d\ln\hat{\sigma}} \approx \left(\frac{0.55}{0.45}\right)^{-1} = 0.82. \tag{A.15}$$

Unauthenticated | Downloaded 07/21/24 03:53 AM UTC

TABLE A2. Vertical-coordinate table used in an annual cycle integration of the UGAMP GCM including physical parameterizations and realistic orography.

Level	$\hat{\sigma}$	$\hat{\theta}$	λ	μ	$a/10^5$	b	$c/10^9$	d
1/2	0.0	—	1.0	0.0	0.0	0.0	0.0	1.0
1 1/2	0.0093	—	1.0	0.0	0.009300	0.0	0.0	1.0
2 1/2	0.0186	705	1.0	0.5	0.018600	0.0	0.0865	0.5
3 1/2	0.0286	625	1.0	1.0	0.028600	0.0	0.1746	0.0
4 1/2	0.0406	550	1.0	1.0	0.040600	0.0	0.1584	0.0
5 1/2	0.0546	500	1.0	1.0	0.054600	0.0	0.1526	0.0
6 1/2	0.0706	460	1.0	1.0	0.070600	0.0	0.1474	0.0
7 1/2	0.0886	430	1.0	1.0	0.088600	0.0	0.1461	0.0
8 1/2	0.1096	403	1.0	1.0	0.109600	0.0	0.1440	0.0
9 1/2	0.1346	379	1.0	1.0	0.134600	0.0	0.1427	0.0
10 1/2	0.1636	360	1.0	1.0	0.163600	0.0	0.1448	0.0
11 1/2	0.1986	344	1.0	1.0	0.198600	0.0	0.1499	0.0
12 1/2	0.2456	329	0.897	1.0	0.220188	0.0254	0.1422	0.103
13 1/2	0.3026	315	0.788	1.0	0.238464	0.0641	0.1323	0.212
14 1/2	0.3716	303	0.675	1.0	0.250953	0.1206	0.1215	0.325
15 1/2	0.4516	295	0.562	1.0	0.253733	0.1979	0.1119	0.438
16 1/2	0.5416	289	0.449	1.0	0.243330	0.2983	0.0999	0.551
17 1/2	0.6359	286	0.343	1.0	0.218270	0.4176	0.0864	0.657
18 1/2	0.7274	285	0.249	1.0	0.180889	0.5465	0.0707	0.751
19 1/2	0.8109	285	0.168	1.0	0.135934	0.6750	0.0531	0.832
20 1/2	0.8819	285	0.102	1.0	0.089701	0.7922	0.0351	0.898
21 1/2	0.9366	285	0.052	1.0	0.049076	0.8875	0.0192	0.948
22 1/2	0.9730	285	0.020	1.0	0.019619	0.9534	0.0077	0.980
23 1/2	0.9923	285	0.003	1.0	0.003208	0.9891	0.0013	0.997
24 1/2	1.0000	—	0.0	1.0	0.0	1.0000	0.0	1.0

We can allow a faster transition rate by making the estimated temperature $\hat{T}$ larger than the actual temperature T, that is, making F positive. This is equivalent to making the estimated potential temperature closer to the mountaintop potential temperature rather than the sea level potential temperature.

(ii) At $\lambda = 1$

$$-\frac{d\lambda}{d\ln\hat{\sigma}} \approx \left(\frac{0.55}{1.0} + \frac{0.3}{0.7} + \frac{1}{0.7}\right)^{-1} = 0.42. \quad \text{(A.16)}$$

Near the sigma levels the rate of transition is limited by the height of the orography. Near the isentropic levels the rate of transition is limited partly by the height of the orography and partly by the relationship between the estimated temperature structure $\hat{T}$ and the actual temperature T.

Comparing (A.15) and (A.16) with (A.10) suggests that a reasonable guess, valid for all $0 \leqslant \lambda \leqslant 1$, might be

$$-\frac{d\lambda}{d\ln\hat{\sigma}} \approx (1.0 + 1.4\lambda)^{-1}. \quad \text{(A.17)}$$

To determine what values of λ to use in practice we might choose the transition rate to be some fraction, ν, say, of the estimated "worst case" marginal transition rate, or more generally

$$-\frac{d\lambda}{d\ln\hat{\sigma}} = \nu(r + s\lambda)^{-1}, \quad \text{(A.18)}$$

for some constants r and s; r and s may be chosen empirically using the above estimates as guidelines. Equation (A.18) can readily be integrated to give

$$\lambda = \frac{-r + [r^2 - 2s\nu(\ln\hat{\sigma} - \ln\hat{\sigma}_0)]^{1/2}}{s}, \quad \text{(A.19)}$$

where $\hat{\sigma}_0$ is the value of $\hat{\sigma}$ at the start of the transition, $\lambda = 0$.

Much less thought has been applied to the transition from isentropic levels to pressure levels. In most cases two half-levels of constant pressure ($\mu = 0$) have been used at the top of the model, including the $p = 0$ half-level, followed by one half-level with $\mu = 0.5$, followed by the uppermost isentropic half-level $\mu = 1$. This has been found to be satisfactory.

The vertical coordinate table listed in Table A2 was constructed using the values $\hat{\sigma}_0 = 0.996$, $\nu = 0.87$, $r = 1.0$, $s = 0.8$ in (A.19) and the values of $\hat{\sigma}$ and $\hat{\theta}$ listed in that table. This vertical-coordinate table has been successfully used in an annual cycle integration of the UGAMP GCM. The zonal mean locations of the model full levels at the start of the integration (15 January) were shown in Fig. 1.

REFERENCES

Black, T. L., 1987: A comparison of key forecast variables derived from isentropic and sigma coordinate regional models. *Mon. Wea. Rev.*, **115**, 3097–3114.

Bleck, R., 1974: Short-range prediction in isentropic coordinates with filtered and unfiltered numerical models. *Mon. Wea. Rev.*, **102**, 813–829.

——, 1984: An isentropic coordinate model suitable for lee cyclogenesis simulation. *Riv. Meteorol. Aeronaut.*, **43**, 189–194.

Unauthenticated | Downloaded 07/21/24 03:53 AM UTC

Bourke, W., 1974: A multi-level spectral model. I: Formulation and hemispheric integrations. *Mon. Wea. Rev.*, **102,** 687–701.

Deavin, D. G., 1976: A solution for boundary problems in isentropic coordinate models. *J. Atmos. Sci.*, **33,** 1702–1713.

Eliassen, A., and E. Raustein, 1968: A numerical integration experiment with a model atmosphere based on isentropic coordinates. *Meteor. Ann.*, **5,** 45–63.

Hoskins, B. J., and A. J. Simmons, 1975: A multi-layer spectral model and the semi-implicit method. *Quart. J. Roy. Meteor. Soc.*, **101,** 637–655.

Hsu, Y.-J., and A. Arakawa, 1990: Numerical modeling of the atmosphere with an isentropic vertical coordinate. *Mon. Wea. Rev.*, **118,** 1933–1959.

Kasahara, A., 1974: Various vertical coordinate systems used for numerical weather prediction. *Mon. Wea. Rev.*, **102,** 509–522.

Phillips, N. A., 1957: A coordinate system having some special advantage for numerical forecasting. *J. Meteor.*, **14,** 184–185.

Robert, A. J., J. Henderson, and C. Turnbull, 1972: An implicit time integration scheme for baroclinic modes of the atmosphere. *Mon. Wea. Rev.*, **100,** 329–335.

Shapiro, M. A., 1975: Simulation of upper level frontogenesis with a 20-level isentropic coordinate primitive equation model. *Mon. Wea. Rev.*, **103,** 591–604.

Simmons, A. J., and D. M. Burridge, 1981: An energy and angular momentum conserving vertical finite difference scheme and hybrid vertical coordinates. *Mon. Wea. Rev.*, **109,** 758–766.

——, B. J. Hoskins, and D. M. Burridge, 1978: Stability of the semi-implicit time scheme. *Mon. Wea. Rev.*, **106,** 405–412.

Trevisan, A., 1976: Numerical experiments on the influence of orography on cyclone formation with an isentropic primitive equation model. *J. Atmos. Sci.*, **33,** 768–780.

Uccellini, L. W., D. R. Johnson, and R. E. Schlesinger, 1979: An isentropic and sigma coordinate hybrid numerical model: Model development and some initial tests. *J. Atmos. Sci.*, **36,** 390–414.

Unauthenticated | Downloaded 07/21/24 03:53 AM UTC